Biosensors and Bioelectronics 62 (2014) 84–89

Contents lists available at ScienceDirect

Biosensors and Bioelectronics

journal homepage: www.elsevier.com/locate/bios

Highly-sensitive liquid crystal biosensor based on DNA dendrimers-mediated optical reorientation

Hui Tan, Xia Li, Shuzhen Liao, Ruqin Yu, Zhaoyang Wu*

State Key Laboratory of Chemo/Biosensing and Chemometrics, College of Chemistry and Chemical Engineering, Hunan University, Changsha 410082, PR China

ARTICLE INFO

Article history:
Received 20 March 2014
Received in revised form
25 May 2014
Accepted 13 June 2014
Available online 20 June 2014

Keywords:
Liquid crystal
Optical reorientation
DNA dendrimer
Hybridization chain reaction
Biosensor

ABSTRACT

A novel highly-sensitive liquid crystal (LC) biosensing approach based on target-triggering DNA dendrimers was developed for the detection of p53 mutation gene segment at the LC–aqueous interface. In this study, the mutant-type p53 gene segment was the target to trigger the formation of DNA dendrimers from hairpin DNA probes by hybridization chain reaction, and the latter as a 'signal enhancement element' further induced the LC reorientation from tilted to homeotropic alignment, resulting in a corresponding optical changes of LC biosensors from birefringent to honeycombed textures or dark framework. The distinct optical reorientational appearances can serve as a characteristic signal to distinguish target concentrations ranging from 0.08 nM to 8 nM. Moreover, these optical phenomena suggest that the LC reorientation is related to the electric-dipole coupling between the adsorbed DNA and LC molecules, the conformational constraints of DNA and the internal electric field induction upon hybridization. This label-free LC biosensing strategy can open up a new platform for the sensitive detection of specific DNA sequences and enrich the application scope of an LC biosensing technique.

1. Introduction

Liquid crystals (LCs) are excellent sensing materials that the intrinsic properties of short-range molecule–molecule interactions and long-range orientational communication can be used to not only amplify but also transduce the biomolecular binding events into macroscopic visible optical signals (Brake et al., 2003; Gupta et al., 1998). The LC biosensing methods using of sandwiching thermotropic LCs between two glass slides have proved to be an effective way to detect specific biomolecules, which are generally based on that the chemical and topographic changes of the well-defined substrates caused by specific biomolecular interactions, such as protein binding events (Clare and Abbott, 2005; Xue and Yang, 2008), DNA hybridization (Chen and Yang, 2010; Yang et al., 2013), and enzymatic reaction (Bi et al., 2009; Tan et al., 2010), can lead to a corresponding changes of the LC orientation. However, the methods usually require multi-step biological immobilizations and washing procedures. Excitingly, the LC-based biosensing methods with the help of amphiphiles (e.g. lipids and surfactants) have recently been achieved simpler detection at the LC–aqueous interface (Chen and Yang, 2013; Hartono et al., 2008; Hartono et al., 2009; Hussain et al., 2014; Khan and Park, 2014; Zuo et al., 2014).

Brake and Abbott (2007) reported that self-assembled phospholipids at LC–aqueous interface could strongly induce the orientational ordering of LCs, the site-specific hydrolysis by phospholipase A_2 could drive the reorganization of the phospholipids and thus trigger reorientational transitions in the LCs, resulting in distinguishable optical appearances easily observed by polarized light microscopy. The method not only mimicked the spatial and temporal distribution of phospholipids during the enzymatic event but also provided a label-free assay for phospholipase activities. The Schwartz group revealed that the changes of cationic surfactant coverage mediated by DNA could lead to the reorientation of LC molecules at the LC–aqueous interface. They speculated that the exposed hydrophobic nucleobases of single-stranded DNA (ssDNA) could intercalate between the surfactant molecules when the ssDNA was adsorbed to the LC–aqueous interface, causing a decreased surfactant coverage and thereby an orientational transition of LCs from homeotropic to planar state. Upon DNA hybridization, the loss of hydrophobic character of ssDNA and the increased charge density of double-stranded DNA (dsDNA) may promote the increased surfactant coverage and thus induce the reorientation of LCs from planar back to homeotropic state (McUmber et al., 2012; Price and Schwartz, 2008). More recently, they found that the conformational change of the adenosine aptamer upon binding the adenosine also could trigger the LC reorientation transition from planar to homeotropic anchoring (Noonan et al., 2013). Nakata et al. (2008) argued that

* Corresponding author. Tel./fax: +86 731 88821989.
E-mail address: zywu@hnu.edu.cn (Z. Wu).

http://dx.doi.org/10.1016/j.bios.2014.06.029
0956-5663/

LC materials like 4-cyano-4′-hexylbiphenyl (6CB) and 4-cyano-4′-octylcycanobiphenyl (8CB) oriented nearly normal to the grooves of dsDNA on dehydrated sheared DNA gels, and the LC–DNA coupling was governed by the dipole–dipole interaction and hydrophobic interaction. These findings shed some light on the construction of new LC-based biosensors as well as understanding of the fundamental mechanism of LCs and biomolecules. But to date, the research of LC-based DNA biosensing technique at the LC–aqueous interface is still unclear. Since the detection of specific DNA sequences plays an important role in molecular diagnostic of genetic diseases and prognosis of cancer therapy and the DNA sequences of interest may be presented in very small amounts (Clark et al., 2009; Cornett et al., 2012; Farjami et al., 2011; Xiang and Lu, 2012), it is necessary to develop a novel DNA technique to meeting these challenges.

Herein, we try to explore the direct LC–DNA sensing mechanism at the LC–aqueous interface and propose a novel signal-enhanced liquid crystal biosensing approach based on target-triggering DNA dendrimers for the highly sensitive detection of specific DNA sequences. Mutations in p53 tumor gene have been implicated in a wide variety of human diseases such as liver cancer, colon disease, and brain tumor (Hussain et al., 2007; Ohgaki et al., 1991); thus it is chosen as a representative model of tumor gene to construct the DNA dendrimers for the signal-enhanced LC biosensors. As shown in Scheme 1, the mutant-type target (target M: a DNA segment with the single-base mutant of the codon 282 from p53 gene) is an initiator of DNA dendrimers, the Y-shaped monomers A and B are the two repeat units of the dendritic monomers structure assembled from six hairpin DNA probes by hybridization chain reaction (HCR). The target M can be detected with high sensitivity by observing the optical reorientation responses of LCs to DNA dendrimers adsorbed at the LC–aqueous interface.

In comparison with the method of single dsDNA-mediated LC reorientation, the method of DNA dendrimers-mediated LC reorientation would possess higher sensitivity because the DNA dendrimers have a large amount of double-helical branches. Moreover, the DNA dendrimers generated by HCR without any ligase or polymerase allow simple and safe preparation to achieve fast mutation gene detection. This LC biosensing strategy would open up a new avenue for highly sensitive detection of specific DNA sequences and enrich the application areas of the LC biosensing technique.

2. Materials and methods

2.1. Materials

Premium grade glass slides were obtained from Xinhua Laboratory Glassware Company (Haimen, China). 200-mesh copper grids (20 μm thickness, 100 μm grid spacing, and 30 μm bar width) were obtained from Zhongjingkeyi Technology Co., Ltd. (Beijing, China). N,N-dimethyl-n-octadecyl (3-aminopropyl) trimethoxy-silyl chloride (DMOAP), and sodium dodecyl sulfate (SDS) were purchased from Sigma-Aldrich. Nematic LC 4-cyano-4′-pentylbiphenyl (5CB) was purchased from Heibei Huajing Scientific and Technological Development Co., Ltd. (Heibei, China). Other reagents were of analytical purity. Ultrapure water was used throughout all experiments.

2.2. Design of target-triggering DNA dendrimers

As shown in Scheme 1, the target M is used as an initiator, and the Y-shaped monomers A and B are the two repeat units of DNA dendrimers assembled from six hairpin DNA probes by HCR. Each hairpin DNA probe has a shared-stem of 15 base pairs enclosing a 45 nucleotide loop and extending an additional 15 nucleotide at the 5′ end. Six shared-stem hairpin DNA probes are designed to ensure that each arm of the stem participates in both hairpin formation and HCR. In the absence of target M, all hairpin probes are in the closed form. However, when the target M is present in the solution, it pairs with the partial loop and the shared stem of hairpin A_1 (HA_1), which undergoes an unbiased strand–displacement interaction to open the hairpin structure. And the opened HA_1 pairs with hairpin A_2 (HA_2) and hairpin A_3 (HA_3) by HCR, resulting in the formation of Y-shaped monomer A. The three single-stranded arms (a, b, c) of monomer A can trigger the Y-shaped monomer B assembled from hairpin B_1 (HB_1), hairpin B_2 (HB_2), and hairpin B_3 (HB_3). Interestingly, monomer A can be regenerated with the help of three newly single-stranded arms (a-, b-, c-) of monomer B.

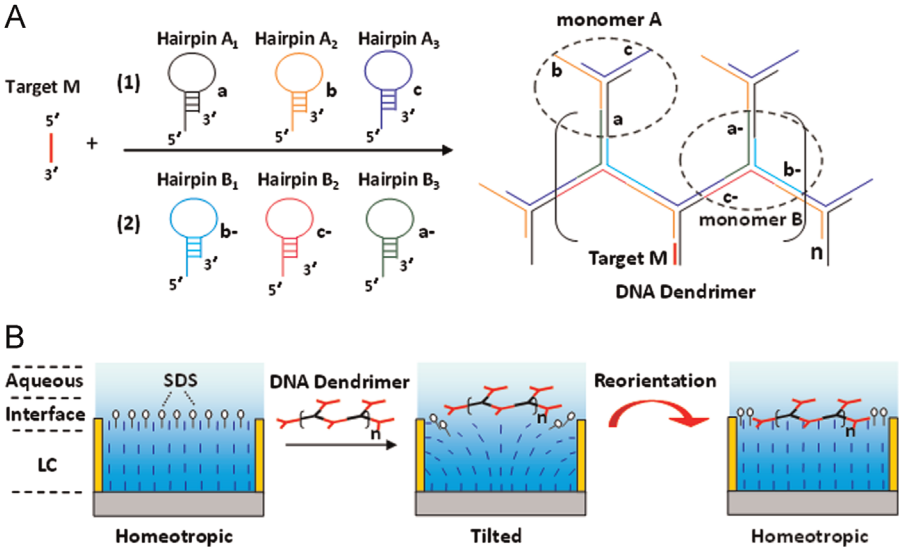

Scheme 1. Illustration of using the DNA dendrimers to enhance the optical signal of LC biosensors. (A) The target-triggering DNA dendrimers are self-assembled from six hairpin probes by HCR. (B) DNA dendrimers induce the orientational changes of sodium dodecyl sulfate (SDS)-doped LCs.

Briefly, each target M can propagate an HCR between alternating A and B monomers to form Y-shaped branches.

All oligonucleotides used in the work were obtained from TaKaRa Biotechnology Co., Ltd. (Dalian, China) and purified by High-Performance Liquid Chromatography. The base sequences of six hairpin DNA probes were firstly optimized by the software at http://mfold.rna.albany.edu to avoid the potential of forming secondary structure within the loop of hairpin DNA probes and to achieve an ideal combination of specificity and thermodynamic parameters. All base sequences are listed in Table S1.

2.3. Cleaning of substrates

The glass slides were cleaned with freshly prepared piranha solution (70% H_2SO_4, 30% H_2O_2) at 80 °C for 1 h to remove all organic contaminants. *Caution: piranha solution reacts violently with organic materials and should be handled with extreme caution; do not store the solution in closed containers!* The glass slides were then rinsed with copious amounts of ultrapure water, dried under a stream of nitrogen, and stored in a 110 °C vacuum oven for at least 3 h before use.

2.4. DMOAP-decoration

Cleaned glass slides were immersed in an aqueous solution containing 0.5% (v/v) DMOAP at room temperature for 5 min and then rinsed with copious amounts of ultrapure water. The DMOAP-coated glass slides were dried under a stream of nitrogen and heated in a 110 °C vacuum oven for 1 h.

2.5. Oligonucleotides hybridization and HCR

All oligonucleotides used in this work were dissolved in a 10 mM Tris–HCl buffer (pH 7.4, 150 mM NaCl, 5 mM $MgCl_2$). The oligonucleotides were firstly heated to 95 °C for 5 min, and then ssDNAs were suddenly cooled to 0 °C for 1 h, while hairpin DNA probes were allowed to cool to room temperature for 12 h before use. For single hybridization, different component concentrations of target mixture containing the target M and the random DNA probe (probe R) were incubated with 450 nM complementary DNA probe (probe C) of target M at 50 °C for 3 h. As for HCR, the target M was firstly incubated with the hairpin probe A_1, A_2 and A_3 at 50 °C for 30 min to form a stable Y-shaped monomer A, then with the hairpin probe B_1, B_2 and B_3 for another 3 h to form a perfect dendritic DNA by HCR. The final concentration of each hairpin probe was 80 nM.

2.6. Preparation of optical cells

The LC material used in this work was a mixture of nematic LC 5CB and SDS. Briefly, a small amount of SDS was doped into the nematic LC 5CB, and sonicated for 10 min before use. The concentration of SDS in 5CB was about 4.50 mM. The clean copper grid was firstly placed onto a surface of DMOAP-coated glass. The LC mixture was then drawn into a 30 μm capillary tube, and then dispensed onto the whole grid via capillary action by contacting the capillary tube to the copper grid, forming an LC layer of approximately 20 μm in thickness. The optical cell was immersed in the 25 μL aqueous solution of interests and kept in a humid environment.

2.7. Polarized light microscope measurements for LC based sensors

The optical appearance of LC cell was examined with a Nikon ECLIPSE 50i POL polarizing microscope (Tokyo, Japan) in transmission mode under crossed polarizers (50% of maximum intensity, 40% open aperture). Homeotropic orientation was determined by the absence of transmitted light during a full 360° rotation of the LC cell. Each experiment was performed with three copper grids and repeated at least five times. Images shown were typical of the results captured by Mshot MD50 digital camera mounted on the microscope (Guangzhou, China).

2.8. UV–vis absorption spectra measurements for DNA and LC 5CB

UV–vis absorption spectra were monitored by a Shimadzu UV-2450 spectrophotometer (Kyoto, Japan) with a 1.0-mm path length quartz cell to investigate the interaction mechanism of DNA and 5CB. The probe C was firstly incubated with target M (or probe R) at 50 °C for 3 h. And then the DNA–5CB interaction systems were prepared freshly in the solution of 80% Tris–HCl and 20% alcohol (v/v) for 10 min at room temperature. The final concentrations of probe C, target M (or probe R) and 5CB were 2.0 μM, 2.0 μM and 20.2 μM, respectively. The slit width was set at 2.0 nm and a slow scan speed was used. The spectra were recorded between 220 and 360 nm at 1.0 nm intervals.

2.9. Atomic force microscope (AFM) measurements for DNA dendrimers

The target M (or wild-type target: a segment with the codon 282 from the wild-type p53 gene, target W) of 3 nM was used to trigger 300 nM hairpin probes self-assembling DNA dendrimers by HCR, then 10 μL of dendritic DNA sample was spotted onto a freshly cleaved mica surface and left to adsorb to the surface for 20 min. Finally, the mica surface was washed with 30 μL 10 mM Tris–HCl buffer and dried by compressed air. AFM images of DNA samples were analyzed by a Dimension 3100 scanning probe microscope (Veeco, America). The tip mounted at the free end of the cantilever was silicon nitride and the tip–surface interaction was minimized by optimizing the scan set-point.

3. Results and discussion

3.1. Effects of ssDNA and dsDNA on LC 5CB orientation

Considering both single-stranded structure and double-stranded structure were presented in the hairpin DNA probes for target-triggering DNA dendrimers, a background signal would possibly accompany due to the cooperative effect of the cationic surfactant/dsDNA complex on LC homeotropic alignment. Therefore, we try to use the classical anionic surfactant SDS as a dopant for the construction of ordered LC cell and further exploration of the potential interactions between LCs and DNA (adsorption of SDS was discussed in Supplementary information, Fig. S1). Following the immersion of the LC-filled copper grids to 450 nM of probe C dissolved respectively in sterilized water and Tris–HCl buffer (pH 7.4, 150 mM NaCl, 5 mM $MgCl_2$), the optical appearances of LC cells showed that some small bright spots appeared in the dark background and then they gradually merged each other into forming colorful birefringent images with the time going on, even though probe C was dissolved in sterilized water (Fig. 1A and B). The results of Fig. 1A indicate that the strong electrostatic repulsions between the hydrophilic head groups of SDS and the phosphate backbones of DNA probably perturb the packing of SDS molecules and thus cause some new sites generated for the direct interactions between 5CB and DNA at the LC–aqueous interface. Moreover, the suitable ionic strength can reduce intermolecular repulsion and enhance the adsorption efficiency of DNA (Fig. 1B).

The analogous responses of Fig. 1C and B at the first few minutes further suggest that the direct interactions between 5CB

and DNA are predominated by the electric-dipole coupling between the phosphate backbones and the highly polarized 5CB but not the hydrophobic interactions from DNA bases (i.e. the hydrophobic character of dsDNA can be neglected upon hybridization), since both ssDNA and dsDNA can be adsorbed to the LC–aqueous interface and cause the dark-to-birefringent texture transition of LC cells. The reorientation optical appearances of Fig. 1C from birefringent texture back to dark framework in the following 41 min indicate that dsDNA can reorganize the arrangement of LCs with dynamically varying from tilted to homeotropic anchoring.

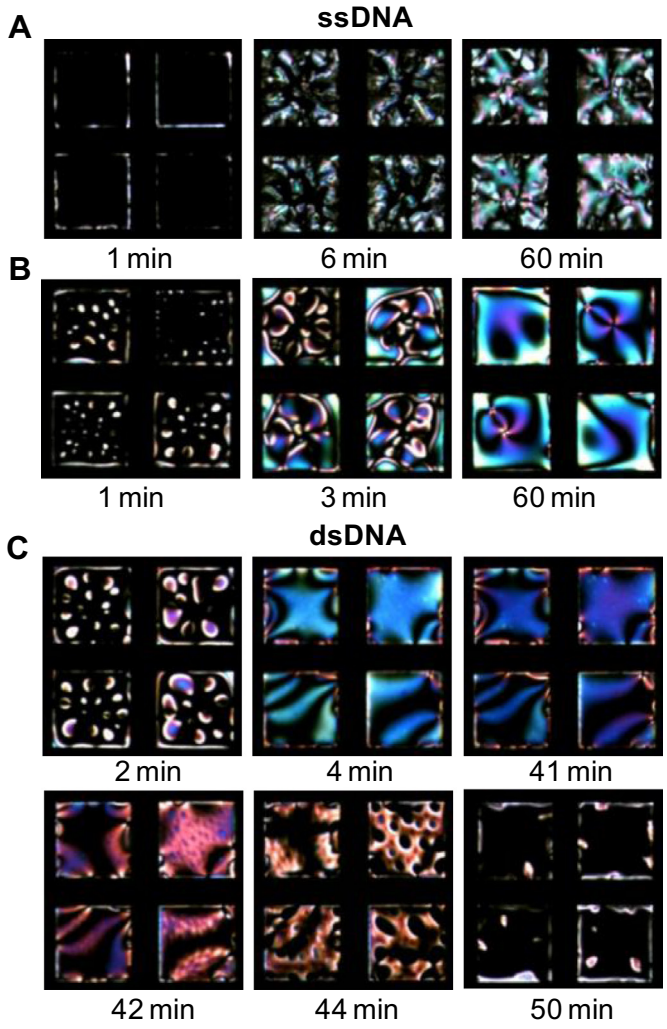

Fig. 1. Optical appearances of the LC cells under crossed polarizers in response to (A, B) ssDNA and (C) dsDNA at the LC–aqueous interface. The probe C was dissolved in (A) sterilized water and (B) Tris–HCl buffer. The dsDNA was generated by hybridizing 450 nM probe C with 450 nM target M. All copper grids used in the work were of 20 μm thickness, 100 μm grid spacing.

3.2. Optical responses of LC 5CB to DNA hybridization

The optical responses of LC 5CB to single DNA hybridization was subsequently investigated by immersing the LC-filled grids in the DNA solutions containing 450 nM probe C and different component concentrations of target M and probe R (the probe C can hybridize with target M but not pair with probe R). It could be found that the surface coverage of black domains mediated by DNA hybridization increased with the increase of target concentration (Fig. 2). The weak and the strong optical responses were observed when the optical response time was fixed at 1 h and the concentrations of target M increased to 100 nM and 200 nM, respectively. The results show that the orientations of LCs close to the LC–aqueous interface are balanced by the interfacial densities of the adsorbed ssDNA and hybridized dsDNA. Moreover, the interfacial density of adsorbed ssDNA would be reduced significantly by single DNA hybridization and thus produce a reorientational response in the optical images.

3.3. Interaction mechanism between LC 5CB and DNA

To further understand what caused the apparent differences between Fig. 1B and C, the ultraviolet–visible (UV–vis) spectrophotometry was used to study the interaction mechanism between LC 5CB and DNA in the solution of 20% alcohol and 80% Tris–HCl (v/v). As can be seen from Fig. S2 that the characteristic absorbance of dsDNA–5CB system decreased obviously (10% hypochromicity) and had a slightly red-shift comparing with that of dsDNA system (Fig. S2A), but the phenomena did not happen in ssDNA–5CB system and its absorbance inversely increased 6% comparing with that of the ssDNA system (Fig. S2B). These spectral effects reflect that the LC 5CB molecule can act as a small molecule intercalating into the dsDNA helix and the intercalation may be a critical factor for the imaging distinction between ssDNA and dsDNA.

More details are described as follows. (1) The adsorption of DNA to LC–aqueous interface disrupts the orientations of LCs from homeotropic to tilted state by direct electric-dipole coupling interaction. We speculate that DNA as a well-known kind of anionic polyelectrolyte can penetrate into the LC side of the LC–aqueous interface for the direct electric-dipole coupling with the highly polarized 5CB and thereby break the initially induction balance of the SDS monolayer, since both ssDNA and dsDNA can be adsorbed to the LC–aqueous interface and lead the dark-to-birefringent images observed at the first few minutes. (2) The reorientation of LC from tilted to homeotropic state is governed by both the conformational constraints of DNA and the internal electric field induction upon hybridization. As the DNA molecules are adsorbed at the interface, the intercalation of the rod-shaped 5CB into the rigid dsDNA helix can assist the dsDNA molecules flat-lying at the interface and thus promote an ordered electrical double layer formed by the negatively charged phosphate backbones of DNA and the positively charged sodium of SDS doped in

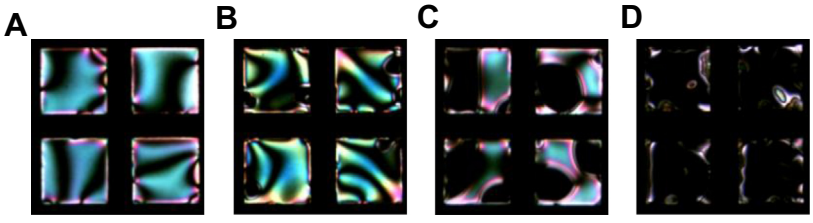

Fig. 2. Optical appearances of the LC cells under crossed polarizers in response to DNA hybridization at the LC–aqueous interface for 1 h. The concentrations of target M/probe R/probe C were (A) 0 nM/450 nM/450 nM, (B) 100 nM/350 nM/450 nM, (C) 200 nM/250 nM/450 nM, and (D) 450 nM/0 nM/450 nM.

the LC 5CB. The internal electric field generated at the LC side of the interface subsequently can drive the tilted-to-homeotropic reorientation transition of the dielectric anisotropic 5CB. Due to the long-range order inherent in LC phases, the tiled-to-homeotropic transition of 5CB molecules would then cause an ordered orientational profile inside the LC cell, making the optical response of LCs to dsDNA from birefringent back to dark at last. However, the ssDNA–5CB coupling is random since the flexible ssDNA is easy to randomly overlap or partially extend at the interface, resulting in the optical response of LCs to ssDNA only birefringent. To some extent, our views are consistent with those of Nakata groups that the steric constraints and the dipolar coupling of the featured DNA films play an important role in the interfacial LC orientations (Nakata et al., 2008).

3.4. Characteristics of target-triggering DNA dendrimers

Since the rigid DNA duplex can induce reorientational anchoring of LCs and the method of single dsDNA-mediated LC reorientations cannot meet the demand for highly sensitive assay, the DNA dendrimers-mediated LC biosensing approach was further developed for the amplification detection of target M (Scheme 1). Here, the atomic force microscope (AFM) was used to characterize the molecular structure of DNA dendrimers. The AFM images of Fig. 3 showed that the DNA dendrimers could not be generated from hairpin DNA probes unless the target M triggered the HCR. Moreover, the arm length of every Y-shaped structure was about 32.4 ± 2.5 nm, which was very close to the theoretically calculated value (30.6 nm) for 90 base pairs of length 0.34 nm each. These results well show that the structures of target-triggering DNA dendrimers are in accord with our design and the proposed method has the potential application in the LC biosensing field.

3.5. Effects of hairpin DNA probes on LC 5CB orientation

The interfacial densities of the adsorbed single-stranded structure and double-stranded structure in the DNAs play a key role in the orientations of LCs and have a great influence on the distinction between positive and negative results. Considering the presence of the double-stranded structure in the stem of hairpin DNA probes, the optical responses of LC 5CB to different concentrations of hairpin DNA probes were investigated. It was found that the birefringent-to-dark negative responses could not be observed until the concentration of each hairpin DNA probe increased to 80 nM with the adsorption time fixed at 4 h (images not shown), indicating the tilted-to-homeotropic orientation transition of LC 5CB was quite weak under the condition. Therefore, the concentration of each hairpin DNA probe at 80 nM was chosen in the latter experiment.

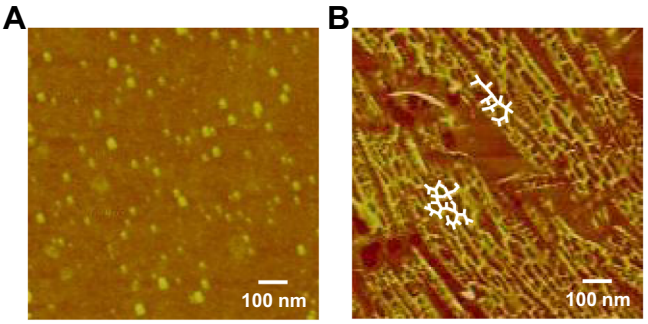

Fig. 3. AFM images of DNA dendrimers triggered by (A) 3 nM target W and (B) 3 nM target M. All hairpin probes were at the concentration of 300 nM. Scale bars: 100 nm.

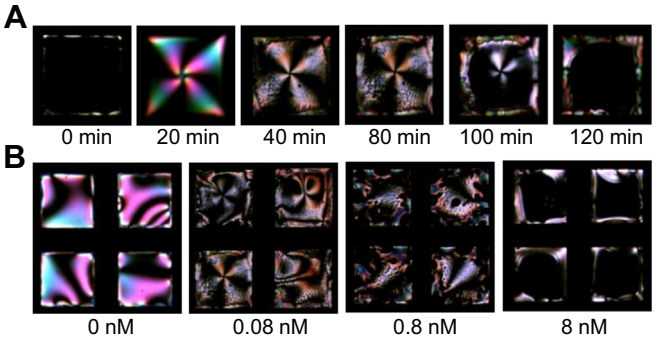

Fig. 4. (A) The DNA dendrimers triggered by 0.08 nM target M induced a dark-to-birefringent-to-honeycombed-to-dark texture changes for LC 5CB varying with time. (B) Optical appearances of the LC cells under crossed polarizers in response to DNA dendrimers triggered by different concentrations of target M, the response time was fixed at 60 min.

3.6. Enhancement of optical reorientation signals by DNA dendrimers

The optical responses of LC 5CB to target-triggering DNA dendrimers were studied by immersing the LC-filled cells in the solutions containing different concentrations of target M and a fixed concentration of each hairpin probe at 80 nM. Interestingly, the optical appearances of LC cells underwent a dark-to-birefringent-to- honeycombed texture transitions for DNA dendrimer triggered by 0.08 nM target M within 40 min, and the honeycombed-to-dark texture changes were observed in the following 80 min (Fig. 4A). However, the optical responses of LC cells to DNA dendrimers triggered by 8 nM of target M or higher concentrations had a dark-to-birefringent-to-dark texture transition within 40 min like those optical appearances of LCs to single DNA hybridization (images not shown). These optical appearances suggest that high interfacial density of DNA dendrimers can significantly enhance the homeotropic reorientation of LC 5CB. It should be noted that the honeycombed textures can act as a characteristic signal to distinguish different concentration levels of target M if the adsorption time of dendritic DNA is fixed at 60 min, since they are stable even the adsorption time increases to 80 min. Obviously, the reorientation response of LC biosensors mediated by DNA dendrimers had a visible change at the concentration of target M low to 0.08 nM and was saturated at 8 nM (Fig. 4B), showing higher detection sensitivity compared with single DNA hybridization.

Although some reports have shown that the concentrated DNA duplexes (e.g. 150 bp) at the concentration of over 160 mg mL^{-1} can exhibit textures of LC phases with pitch in the visible range, up to a few microns or longer (Nakata et al., 2007; Zanchetta et al., 2010), the honeycombed textures here may be attributed to the LC 5CB intercalation, the electric-dipole coupling and the steric constraints of rigid DNA dendrimers. Moreover, the long-range orientational order and the optical anisotropy of LC 5CB can further amplify and transduce the DNA dendrimers into the macroscopic optical signals in the 1- to 20-μm thickness of bulk LC phase.

3.7. Selectivity of DNA dendrimers-mediated LC biosensor

The selectivity of the LC biosensors based on DNA dendrimers was investigated by observing the reorientation responses of LC cells to the target M and the target W with the same concentrations. As shown in Fig. S3A and B, the reorientational signal of the target W-triggering DNA dendrimers was significantly weaker than that for target M-triggering DNA dendrimers. The result

suggests that the LC biosensors based on DNA dendrimers has good selectivity.

4. Conclusion

In summary, we have investigated the sensing mechanisms of DNA-mediated LC reorientation at the LC–aqueous interface and proposed a novel signal-enhanced LC biosensing method based on target-triggering DNA dendrimers for the label-free and sensitive detection of p53 mutation gene segment. Results showed that the homeotropic-to-tilted ordering transition of LCs was related to the electric-dipole coupling between the adsorbed DNA and LC molecules, and the tilted-to-homeotropic reorientation of LCs was governed by both the conformational constraints of DNA and the internal electric field induction upon hybridization. Specifically, the distinct optical reorientational signals of the birefringent to honeycombed textures or dark framework induced by DNA dendrimers can serve as a characteristic signal to distinguish target concentrations ranging from 0.08 nM to 8 nM. This well revealed that the DNA dendrimer could be used as an excellent signal enhancement element for inducing the LC reorientation at the LC–aqueous interface. The combination of LC reorientation and DNA dendrimer signal amplification contributed a label-free and sensitive method for the detection of DNA concentration as low as 0.08 nM. This LC biosensing strategy is expected to be a promising means for the study of various DNA (including aptamer)-based interactions, such as base-pairing interaction, metal–base interaction and protein–aptamer binding events (Chen and Zeng, 2013; Liu et al., 2012; Zhang et al., 2012).

Acknowledgments

This research was financially supported by the International Scientific and Technological Cooperation Projects of China (2012DFR40480) and the National Natural Science Foundation of China, China (21175037 and 21277042).

Appendix A. Supplementary information

Supplementary data associated with this article can be found in the online version at http://dx.doi.org/10.1016/j.bios.2014.06.029.

References

Bi, X., Lai, S.L., Yang, K.-L., 2009. Anal. Chem. 81, 5503–5509.
Brake, J.M., Abbott, N.L., 2007. Langmuir 23, 8497–8507.
Brake, J.M., Daschner, M.K., Luk, Y.-Y., Abbott, N.L., 2003. Science 302, 2094–2097.
Chen, C.-H., Yang, K.-L., 2010. Langmuir 26, 1427–1430.
Chen, C.-H., Yang, K.-L., 2013. Sens. Actuators B Chem. 181, 368–374.
Chen, J., Zeng, L., 2013. Biosens. Bioelectron. 42, 93–99.
Clare, B.H., Abbott, N.L., 2005. Langmuir 21, 6451–6461.
Clark, A.W., Glidle, A., Cumming, D.R., Cooper, J.M., 2009. J. Am. Chem. Soc. 131, 17615–17619.
Cornett, E.M., Campbell, E.A., Gulenay, G., Peterson, E., Bhaskar, N., Kolpashchikov, D.M., 2012. Angew. Chem. 124, 9209–9211.
Farjami, E., Clima, L., Gothelf, K., Ferapontova, E.E., 2011. Anal. Chem. 83, 1594–1602.
Gupta, V.K., Skaife, J.J., Dubrovsky, T.B., Abbott, N.L., 1998. Science 279, 2077–2080.
Hartono, D., Bi, X., Yang, K.L., Yung, L.Y.L., 2008. Adv. Funct. Mater. 18, 2938–2945.
Hartono, D., Lai, S.L., Yang, K.-L., Yung, L.-Y.L., 2009. Biosens. Bioelectron. 24, 2289–2293.
Hussain, S., Schwank, J., Staib, F., Wang, X., Harris, C., 2007. Oncogene 26, 2166–2176.
Hussain, Z., Zafiu, C., Küpcü, S., Pivetta, L., Hollfelder, N., Masutani, A., Kilickiran, P., Sinner, E.-K., 2014. Biosens. Bioelectron. 56, 210–216.
Khan, M., Park, S.-Y., 2014. Anal. Chem. 86, 1493–1501.
Liu, X., Aizen, R., Freeman, R., Yehezkeli, O., Willner, I., 2012. ACS Nano 6, 3553–3563.
McUmber, A.C., Noonan, P.S., Schwartz, D.K., 2012. Soft Matter 8, 4335–4342.
Nakata, M., Zanchetta, G., Buscaglia, M., Bellini, T., Clark, N., 2008. Langmuir 24, 10390–10394.
Nakata, M., Zanchetta, G., Chapman, B.D., Jones, C.D., Cross, J.O., Pindak, R., Bellini, T., Clark, N.A., 2007. Science 318, 1276–1279.
Noonan, P.S., Roberts, R.H., Schwartz, D.K., 2013. J. Am. Chem. Soc. 135, 5183–5189.
Ohgaki, H., Eibl, R.H., Wiestler, O.D., Yasargil, M.G., Newcomb, E.W., Kleihues, P., 1991. Cancer Res. 51, 6202–6205.
Price, A.D., Schwartz, D.K., 2008. J. Am. Chem. Soc. 130, 8188–8194.
Tan, H., Yang, S., Shen, G., Yu, R., Wu, Z., 2010. Angew. Chem. 122, 8790–8793.
Xiang, Y., Lu, Y., 2012. Anal. Chem. 84, 1975–1980.
Xue, C.-Y., Yang, K.-L., 2008. Langmuir 24, 563–567.
Yang, S., Wu, C., Tan, H., Wu, Y., Liao, S., Wu, Z., Shen, G., Yu, R., 2013. Anal. Chem. 85, 14–18.
Zanchetta, G., Giavazzi, F., Nakata, M., Buscaglia, M., Cerbino, R., Clark, N.A., Bellini, T., 2010. Proc. Natl. Acad. Sci. U.S.A 107, 17497–17502.
Zhang, G., Lin, W., Yang, W., Lin, Z., Guo, L., Qiu, B., Chen, G., 2012. Analyst 137, 2687–2691.
Zuo, F., Liao, Z., Zhao, C., Qin, Z., Li, X., Zhang, C., Liu, D., 2014. Chem. Commun. 50, 1857–1860.